Local FRP Reinforcement of Existing Timber Beams

Marco Corradi*

Department of Mechanical and Construction Engineering, Wynne Jones Building, Northumbria University, NE1 8ST, Newcastle upon Tyne (United Kingdom) and

Department of Engineering, Perugia University, Via Duranti, 92 06125, Perugia (Italy)

Chandra Mouli Vemury

Vemury Structural Consultancy Ltd, Newcastle upon Tyne (United Kingdom)

Vikki Edmondson, Keerthan Poologanathan, Brabha Nagaratnam

Department of Mechanical and Construction Engineering, Wynne Jones Building, Northumbria University, NE1 8ST, Newcastle upon Tyne (United Kingdom)

* corresponding author, marco.corradi@northumbria.ac.uk, Tel. +44 (0)191 227 3071,

KEYWORDS: Timber beams, polymeric resins, FRP sheet, reinforcement.

ABSTRACT

Timber beams in historic buildings tend to display signs of mechanical degradation in the form of large bending deformations and reduced capacity, often caused by timber defects. This paper addresses the assessment of the bending resistance of small timber beams subjected to static loads, before and after they have been reinforced using Fibre Reinforced

Polymer sheets (FRP). The retrofitting of timber elements using FRP is not a new technique and several experimental research programmes have demonstrated that it is possible to increase the bending capacity of wood beams using FRPs. It is well understood that premature bending failure in timber beams and large bending deformations under loading are often caused by defects (e.g. splay or dead knots, shakes, etc.). This paper presents an experimental work where FRP sheets have been locally applied in the area where defects were noted. The structural response of locally reinforced timber elements when subjected to flexural loading was studied using a series of experiments. The results from the bending tests demonstrate that it is possible to partially restore the bending capacity of defective timber beams with the application of the reinforcement method proposed in this paper.

1. INTRODUCTION

Timber is a natural composite material which bears similarities with some modern Fiber Reinforced Polymers (FRP). Timber fibres are made of cellulose embedded in a matrix of hemicellulose and lignin [1]. The longitudinal tensile strength (i.e. along the grain strength) of timber fibres is one of the mechanical properties of interest to structural engineers [2]. Timber has been used as a construction material since thousands of years. The unique mechanical properties of timber have made it ideally suited for being used as the material of choice for structural elements in roof and flooring systems. Traditional building construction in Europe and the rest of the world had often consisted of flooring systems made of one-way spanning timber floors supported by softwood or hardwood joists and roofing frames built from timber trusses [3-4]. Timber beams were typically used for ground floors, or to bridge the space above a room and to provide structural support. These timber structures were normally subjected to bending (transversal) loads. However, timber structural elements are common not only in centuries old, historic, or listed buildings, but also in more recent structures built worldwide.

Despite being a popular construction material, timber may have various kinds of defects which adversely affect its mechanical performance under bending loads. Knots in timber cause cracking and significantly affect beams' bending stiffness and capacity. When knots are localised at the tension side of a beam, they significantly reduce the engineering properties (Fig. 1). It is well known that the weakening effect caused by the presence of knots is much more serious when timber is subjected to parallel-to-grain bending or tension rather than compression forces.

Creep deformation is another critical problem of timber beams: an unsatisfactory creep response is often facilitated by the presence of knots, where local cracks may occur with time. Cracks and shakes in the areas near the knots are more likely to occur than in the rest of the timber beam, also considering the stress concentration at the reduced beam cross-sections where knots are. However, it has been demonstrated that FRP-reinforcement can effectively reduce the creep behavior of timber beams [5-7].

Structural engineers are often asked to design remedial measures to repair or reinforce timber roof and floor elements weakened by the presence of knots. It would be difficult to find timber beams without knots because knots are the effect of branching of the trees. A well-known quality control method of assessing timber structural elements is to check the 'R' ratio, which is the ratio of the diameter of a knot d and the smallest dimension of the timber beam (b_W or h_W). According to Giordano [8], timber tensile strength reduces by 24% and 46.2% for 1/5<R<1/3 and 1/3<R<1/2, compared to when this ratio is smaller than 1/5, respectively (Fig. 2). Numerous international standards use visual strength grading, based on the dimensions and density of defects such as knots in timber [9-10].

Due to the introduction of new building design codes and structural safety requirements in many European countries, pre-existing timber structures in these countries must, now, satisfy much more onerous design load demands than the originally estimated loads at the time of their design and construction. As a consequence of this, a large number of timber structures do not meet the current strength requirements and, hence, require reinforcement interventions or face the prospect of demolition.

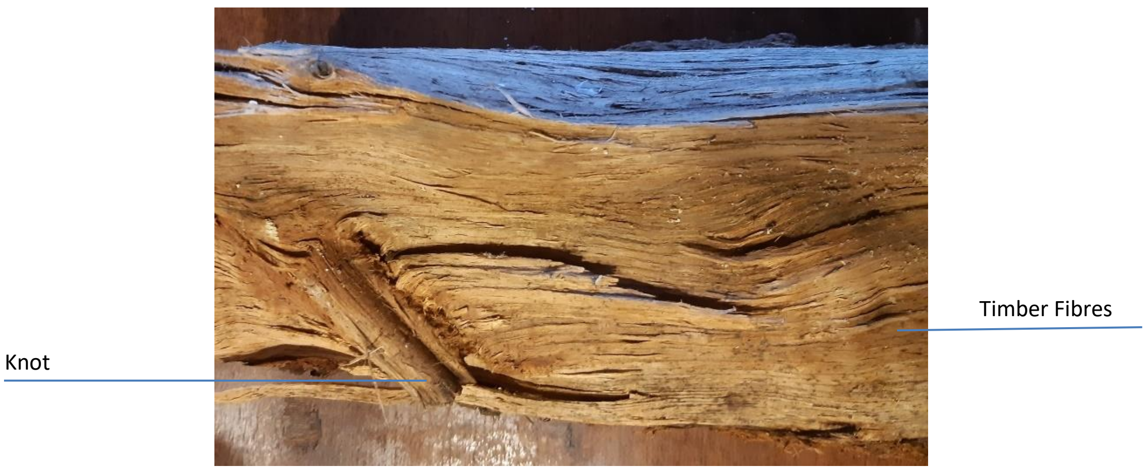

Figure 1. A section of a timber beam showing the devastating effect of a knot: it can be noted that timber fibres are interrupted by the presence of a knot.

For a long period of time in the last century (1960 - 90s), the generally adopted solution was the demolition of the old timber structures and their replacement with Reinforced Concrete (RC) structural frames or plates [11-12]. The aesthetic value of the buildings of historic significance highly suffers when the original timber elements are replaced with RC members. In parts of southern Europe, recent earthquakes have demonstrated that masonry buildings suffer significant damage when the timber floor systems or roof trusses are replaced with RC elements (Fig. 3). This is the inevitable consequence of the increase of mass and low compatibility between the original masonry material and the newly introduced RC.

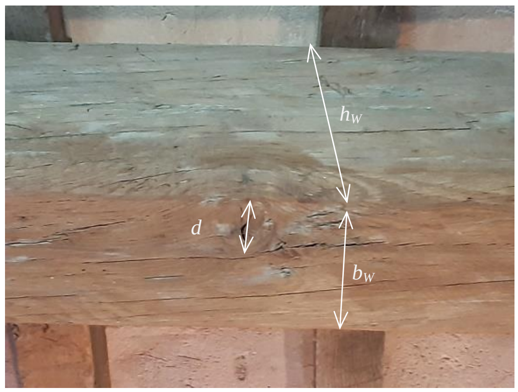

Figure 2. Example of a solid timber beams with knots, and the method of calculation of ratio R (external diameter of a knot *d* / beam smallest dimension h_W or b_W). This weakening effect is more serious when the lumber is subjected to tensile forces (typically the beam tension side).

Figure 3. Effect of earthquakes on historic buildings where timber roof beams were replaced with RC elements.

Instead of removing defective timber structural members, they may be retrofitted using metal reinforcements [13-15] or new advanced polymers elements [16-18]. A considerable amount of research has been conducted in the last two decades using FRP as reinforcement material applied on the tension and compressions sides of timber beams. The use of glued-in rods [19-21], FRP plates [22-23], mechanical attached FRP elements [24-25], FRP bonded-to-timber [26-27] and Glass Reinforced Plastic (GRP) pultruded profiles are examples of some of the innovations in timber engineering research. These investigations have clearly shown that the application of FRPs can enhance the strength and ductility of timber beams. The use of FRP sheets is to be preferred as "it confines local rupture and bridges local defects in the timber and this has a considerable effect on the strength properties" [28]. Furthermore, FRP is a cost-effective alternative to timber beams demolition and to other retrofit solutions such as stainless steel. Its benefits as a retrofit material include quick and lower cost installation, versatile design capabilities and chemical corrosion resistance.

Validation of the reinforcement effect of timber beams with FRP sheets was demonstrated by Dziuba [29], Fiorelli and Dias [30], Buell and Saadatmanesh [31], Borri et al. [32], Nianqiang and Weixing [33], Plevris and Triantafillou [34] and Bashandy et al. [35].

With regards to the reinforcement of glulam (layered timber beams) elements with FRPs, pioneeristic studies were carried out by Triantafillou [36] and Johns and Lacroix [37]. The research undertook by Alam et al. [38] and Vahedian et al. [39] is also interesting: full scale beams have been reinforced using FRP sheets or bonded-in reinforcements, demonstrating the capacities and added operational value of composite materials in this area.

The application of FRP reinforcement is often achieved by using an organic adhesive, i.e. an epoxy or a polyester resin (Fig. 4a). The resin has a critical role as it must transfer, by shear, the stresses between the timber beam and the composite fibres. The FRP is usually bonded to the whole surface subjected to tensile stresses (beam tension side) (Fig. 4). Apart from aesthetic considerations, the application of large sheets of composite materials may obstruct transpiration and evaporation of moisture in the timber material. These conditions could lead to the formation of areas with a high level of moisture content, creating a risk of biotic attack (fungi, insects, etc.).

 (a)  (b)

 (c)

Figure 4. Different retrofitting methods using FRPs: (a) FRP sheets; (b) FRP pultruded elements at the compression side; (c) CFRP laminae.

In this paper, we propose to reinforce timber beams against localised defects using small pieces of FRP sheets. These are applied only in the areas where serious defects are located.

2. TIMBER BEAMS

This paper presents an experimental study of the use of Carbon FRP sheets (CFRP) to reduce the weakening effect of defects (knots) located on the tension side of solid timber beams. This research is only focused on the effect of knots, and did not account for other defects as it is well accepted that knots are one of the most serious type of defect in timber beams subjected to bending loading. However, the proposed reinforcement method could be also effective to prevent or delay failure (cross-grained tension failure) of timber beams with a large grain deviation.

Non-defective and defective timber beams were tested in bending with and without the CFRP reinforcement. Two types of defective timber beams were considered: (1) beams with a knot (natural defect) located about the mid-span on the tension side, and (2) artificially damaged beams. The artificial damage was in the form of a transversal cut of 5 mm depth on the tension side at mid-span of the beams. The transversal cut was applied only on small beams. CFRP sheets were epoxy glued over the natural and artificial defects and tested in bending. A total of 36 beams were tested in four-point bending: 24 small beams (27.5 x 27.5 x 500 mm) and 12 timber rafters (100 x 100 x 2000 mm) (large beams). The beams were made from firwood with an approximate density [40] of 449.5 and 421.2 kg/m^3 for small and large beams, respectively (Tab. 1).

Table 1. Rheological and mechanical characteristics of timber beams.

Type of fibres	Small Beams	Large Beams
Wood species	Firwood (*Abies Alba*)	Firwood (*Abies Alba*)
Beam dimensions (mm)	27.5x27.5x500	100x100x2000
Weight density (kg/m^3)	449.5	421.2
Weight density CoV (%) [40]	5.57	3.79
Origin	same batch	same batch
Moisture content (%) [41]	11.1	10.9
Moisture content CoV (%)	8.5	11.3
Compressive Strength* (MPa) [42]	27.3	24.1
Compressive Strength* CoV (%)	16.1	18.7

* parallel to grain, CoV = Coefficient of Variation

Both types of timber beams were subject to visual grading prior to testing: all beams presented a grain deviation smaller than 15°. Grading was only based on the dimension of the knots located on the beam's tension side: the R-ratio of "non-defective" beams was always < 1/5, while this was in the range 1/5 – 1/2 for "defective" beams.

Of the 24 small beams, 5 were non-defective and 19 defective (11 beams with a natural defect (knot) and 8 beams with an artificial defect, both located on the tension side). The 19 defective small beams were divided in two groups: 8 beams which were tested without CFRP reinforcement (5 beams with a natural defect, 3 beams with an artificial one) and 11 reinforced with a CFRP sheet each, applied locally over the defect (6 beams with a natural defect, 5 beams with an artificial one).

Similarly, for the 12 large beams, three groups of 4 beams each were formed containing non-defective, defective-unreinforced and defective-CFRP-reinforced, respectively.

3. TEST SET UP

A steel jig was mounted onto the electro-mechanic dynamometer (Fig. 5a) for the testing of small beams. For large beams, a 500kN oleo-dynamic actuator was used. To achieve four-point bending a steel spreader beam was used (Fig. 5b). The distance between the two loading points was about 1/3rd of the span (460 and 1900 mm, for small and large beams, respectively) (Fig. 6). The tests were displacement controlled, with the cross head of the electro-mechanic dynamometer or actuator, moving at 5 mm/min. Bending loading continued until either the loading instrument detected a sudden jump in loading indicating failure or when significant damage was observed. To avoid crushing of timber, supports and loading points made of steel cylinders with a diameter of 20 mm were used for tests on small beams.

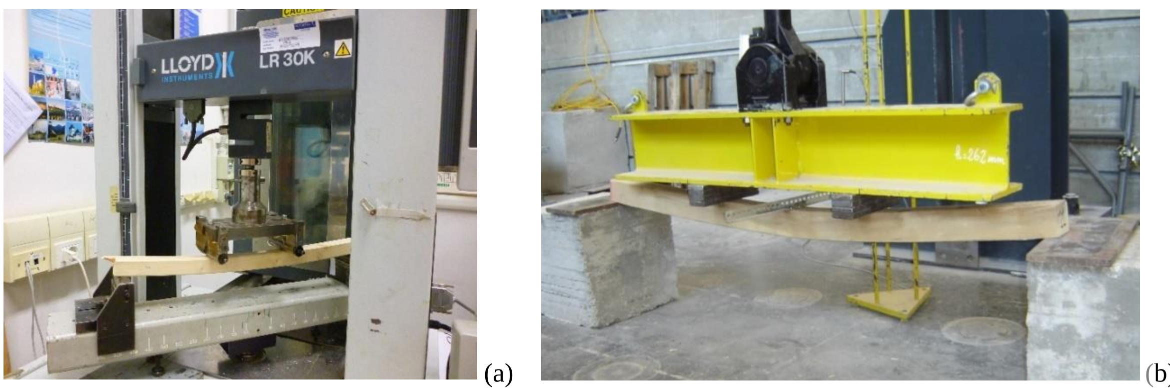

Figure 5. Experimental testing set up: (a) small beams; (b) large beam (rafters).

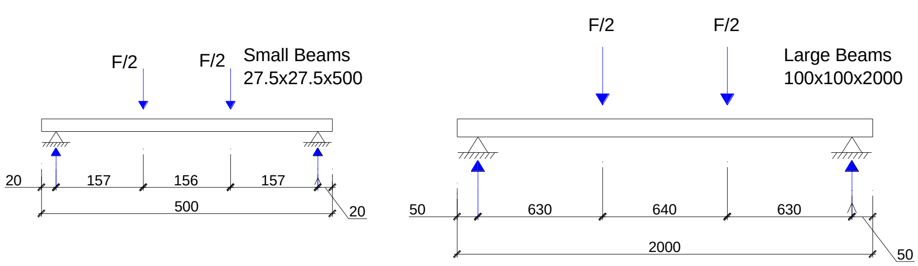

(a) (b)

Figure 6. Four-point bending: (a) small beams; (b) large beam (rafters) (dimensions in mm).

Testing of both unreinforced, defective and reinforced beams was carried out using the same experimental procedure as in the initial tests. This was done in order to provide a fair comparison of the beam capacity.

4. REINFORCEMENT METHOD

Both artificially damaged and naturally defective timber beams were reinforced using small sheets of CFRP. The reinforcement was made of unidirectional carbon fibres, which were epoxy glued to the timber specimens (Fig. 7). The nominal thickness and the tensile strength of the carbon sheet were 0.165 mm and 3324 MPa, respectively [43]. Table 2 reports the mechanical properties of the CFRP sheet used for reinforce along with the mechanical properties of the glass fibres (GFRP) initially used for bond tests.

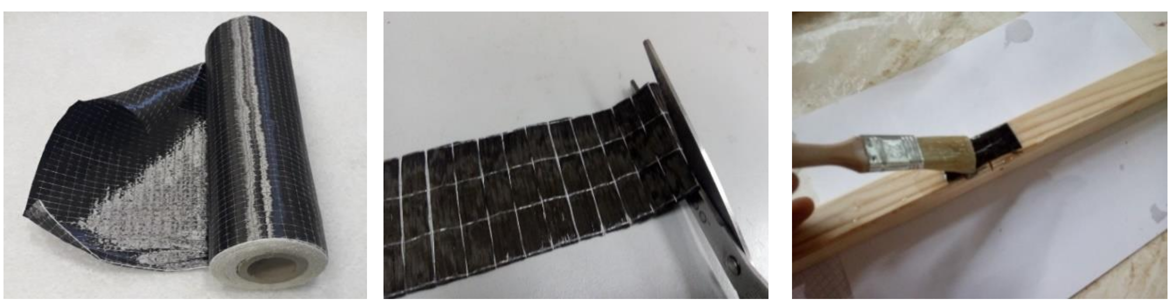

(a) (b) (c)

Figure 7. (a) Carbon unidirectional sheet, (b) Cutting to dimensions, (c) Application of the epoxy resin.

The surface of the defective beams was carefully prepared for reinforcement. This involved the removal of any loose debris and dust from the surface of the beams. The epoxy resin was then applied using a paint brush only on timber surface to avoid penetration into the artificial cut. To ensure uniform conditions, CFRP was applied to all beams on the same day at a room temperature of 20 °C and were left to cure. According to the manufacturer's guidelines, the resin should be left for 72 hours to be fully cured. However, the beams were given a total of 7 days to cure in order to ensure maximum effectiveness of the reinforcement.

Table 2. Results of mechanical characterization tests [43]: CFRP and GFRP (CoV= Coefficient of Variation).

Type of fibres	Carbon	Glass
Orientation	Unidirectional	Unidirectional
Number of Tested Samples	10	10
Dry Fibre Thickness (mm)	0.165*	0.118*
Weight Fibre Density (kg/m^2)	0.300	0.300
Matrix Type	Epoxy	Epoxy
Tensile Strength (MPa) - (CoV) (%)	3324^+ - (18.1)	1571^+ - (13.3)
Young's Modulus (MPa) - (CoV) (%)	312200^+ – (19.2)	77432^+ – (11.1)

* equivalent thickness, based on the total carbon content, + nominal

The carbon fibre was impregnated using a bi-component epoxy resin. This also served to glue the fibres to the timber. The epoxy resin is commercialized by the Italian company Kimia, under the brand name Kimitech-ep-in. The resin is a low-viscosity, transparent, bi-component product, with a compressive strength of 65 MPa, and a tensile strength of 30.4 MPa (data from the product specification sheet). The weight density of the epoxy resin is 1.08 g/cm^3.

The unidirectional CFRP sheet used for reinforcement was 50 x 27 and 140 x 80 mm, for small and large timber beams, respectively, where both carbon fibres and the larger sheet dimension (50 and 140 mm) were oriented along the beam longitudinal axis. CFRP sheet was centered about the natural or the artificial defect.

5. EXPERIMENTAL RESULTS

5.1 Analysis of the wood-to-FRP bonding

To study the mechanism of bond transfer of externally bonded FRP sheets to timber, a preliminary experiment was carried out in the laboratory. Three types of seasoned timber were used (fir, chestnut and oak wood) with a moisture content ranging between 9.1 and 13.7% [44]. Timber samples (60 x 10 x 20 mm in dimensions) were reinforced using Carbon and Glass FRP (CFRP and GFRP, respectively). A total of 30 samples were tested.

Bond tests were carried out according to the double-lap push-pull shear test, also known as the double-shear push (Yao et al. 2004). Tests were conducted using a 30kN-cell universal testing machine at the Structures laboratory of the University of Perugia, Italy. Double-lap test arrangement has some limitations: in general, it is difficult to reproduce specimen symmetry and thus ensure equal distribution of the tensile load between the two ends of the FRP sheet. To overcome this problem, a single FRP unidirectional sheet was used (10 x 160 mm in dimensions). The two ends of the sheet were bonded to the timber surfaces (10 x 20 mm). A steel reel was used to apply the tensile load and to ensure an equal distribution of the tensile loads to the two bonded areas.

Another problem of the double-lap test set-up is the misalignment of the load on the specimens, causing out-of-plane stresses on the bonded areas. Clearly, this is an important limitation to account for, and caution should be shown when test results are interpreted. However, both specimen’s non-symmetry and misalignment of the load are likely to affect tests results, causing an underestimation of the FRP-to-timber bond strength. However, when bond test results are used for design purposes, this underestimation is in a sense, beneficial to structural safety.

The normal stress in the FRP was calculated (force/sectional area) and, for a limited number of specimens, axial strain was measured using strain gauges installed on each of the two reinforcing bonded FRP ends. All of the readings were saved on a computer by means of Spider8 data acquisition system. Specimens were tested under displacement control at a rate of 0.2 mm/min. The universal testing machine also measured the relative movements between the clamps. Force, displacement and strain (where available) and time were recorded with a frequency of 4 Hz.

While loading, cracks did not initiate in any of the timber specimens irrespective of the timber species (Fir, Chestnut or Oak). The load vs clamp-relative-movement relationship was essentially linear up to failure. For high levels of load, a reduction in stiffness was occasionally noted, but this was the consequence of tensile rupture of a few of the composite fibres.

The predominant failure mode was by peeling (for Firwood) or by FRP debonding (for Chestnut and Oak wood) (Tab. 3) (Fig. 8). These modes of failure were sudden, noisy and brittle. The corresponding average failure loads ranged between 1664 N (GFRP-reinforcement of Chestnut specimens) to 2040 N (CFRP-reinforcement of Oak specimens): these values correspond to a range of bonding strengths of 8.32 and 10.2 MPa. The difference in the failure load between CFRP and GFRP reinforcement is quite small. For Chestnut and Oak wood, the load capacity is mainly governed by the bonding properties of the epoxy-resin, while, for Fir-specimens, where peeling failure was more frequent, by the wood tensile strength (perpendicular-to-grain).

Finally, by considering the ratio between the maximum FRP tensile stresses (at debonding) and tensile strengths (0.35 for carbon, and 0.92 for glass fibres), it can be noted that there was a very efficient use of the GFRP material. However, given the usual factors of safety adopted in Civil Engineering (typically ranging between 1.5 and 3), and the higher value of Young's modulus of the Carbon fibres, it was decided to only use CFRP sheets for reinforcement of timber beams.

Table 3. Results of bonding tests.

	Firwood	Chestnut	Oak wood
Number of tested samples	10	10	10
Failure Load			
CFRP-reinforcement (N)	3652 (13.1)	3904 (14.3)	4080 (9.2)
GFRP-reinforcement (N)	3572 (18.2)	3328 (15.1)	3640 (11.1)
Bonded surface (mm)	20x10	20x10	20x10
Bonding strength			
CFRP-reinforcement (MPa)	9.13 (13.1)	9.76 (14.3)	10.20 (9.2)
GFRP-reinforcement (MPa)	8.93 (18.2)	8.32 (15.1)	9.13 (11.1)
Corresponding CFRP tensile stress (MPa)	1107 (13.1)	1183 (14.3)	1236 (9.2)
Failure mode	Peeling / Debonding	Debonding	Debonding

CoV in ( )

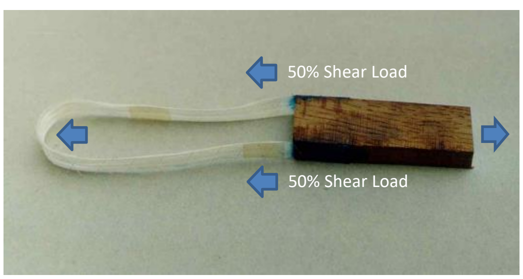

Figure 8. Double-lap push-pull shear test.

5.2 Bending tests of non-defective beams

It is important to highlight that the "non-defective" beams were solid timber elements with knot defects which were limited in number and dimensions (R<1/5). These beams were selected, using visual inspection, from a single batch of fir beams. The results of the initial series of tests carried out on 5 (undamaged) fir beams of small dimensions are presented in Figure 9. The average bending capacity was 2.691 kN, corresponding to a bending strength 61.2 MPa. A coefficient of variation of 13.1% was obtained for the strength. This variation is most likely caused by small defects (mainly a deviation of grain).

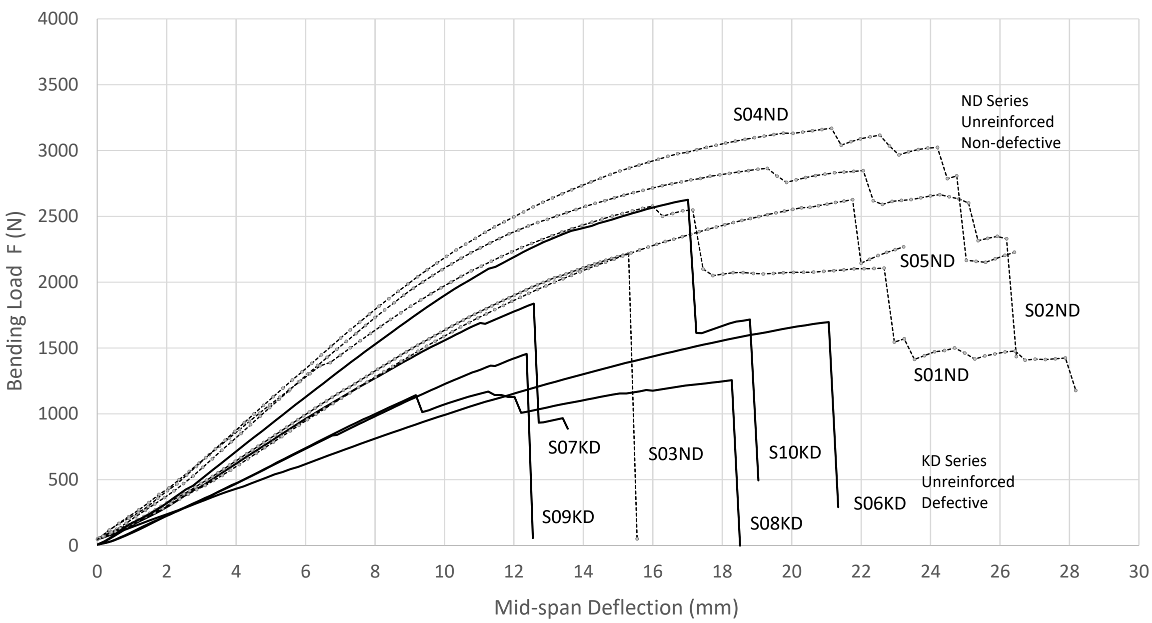

Figure 9. Four-point bending tests (simply supported ends): load versus mid-span deflection for unreinforced non-defective (ND Series) and defective (KD Series) small beams.

During testing it was found that the non-defective beams generally failed in two different ways: 1. Tensile failure of the timber fibres on the beam tension side (straight-grained beams) (Fig. 10a) 2. Fracture propagating along the grain of timber (i.e. cross-grained tension failure) (Fig. 10b) when the grain deviation was larger than 10°. The latter failure mode is one of the most relevant failure mechanisms producing a brittle failure behaviour when subjected to excessive shear and tensile stresses perpendicular to the grain.

Tests results were processed and the bending strength f_m evaluated thus:

$$f_m = a\frac{F_u}{2W} \quad (1)$$

where F_u is the ultimate load (N), a is the distance between the point of application of the load and the nearest support (mm) and W is the modulus of resistance of the section (mm^3) about the neutral axis.

The flexural stiffness $k_{1/3}$ of the beams was also measured, using:

$$k_{1/3} = \frac{F_u}{3s_{1/3}} \quad (2)$$

where $s_{1/3}$ is the mid-span deflection corresponding to a bending load of 1/3 F_u.

Table 4. Results of bending tests for small beams.

	Beam Number	R-ratio value*	F_u Maximum Load (N)	Failure mode	f_m Bending Strength (MPa)	Strength Loss (%)	Flexural Stiffness $k_{1/3}$ (N/mm)
Non Defective (ND) Beams	S01ND	0.12	2865	(1)	65.2	-	212.2
	S02ND	0.18	2578	(1)	58.6	-	214.8
	S03ND	0.17	2218	(2)	50.4	-	164.3
	S04ND	0.11	3169	(1)	72.1	-	224.7
	S05ND	0.17	2627	(2)	59.7	-	159.2
	Mean (CoV)		*2691 (0.131)*		*61.2*	-	*195.0 (0.158)*
Defective Beams (Knot Defect, KD)	S06KD	0.41	1697	(3)	38.6	36.9	105.8
	S07KD	0.35	1838	(3)	41.8	31.7	156.3
	S08KD	0.41	1256	(3)	28.6	53.3	116.2
	S09KD	0.45	1456	(3)	33.1	45.9	118.4
	S10KD	0.22	2627	(3)	59.7	2.4	182.4
	Mean (CoV)		*1775 (0.296)*		*40.4*	*34.1*	*135.8 (0.238)*
Defective Beams (Artificial Defect, AD)	S11AD	-	1035	(4)	23.5 [32.2]	61.5	123.3
	S12AD	-	1520	(4)	34.6 [47.3]	43.5	151.7
	S13AD	-	1326	(4)	30.2 [41.3]	50.7	152.4
	Mean (CoV)		*1294 (0.189)*		*29.4 [40.3]*	*51.9*	*142.5 (0.117)*
Defective (Knot Defect) CFRP Reinforced Beams (KD_R)	S14KD_R	0.34	2489	(1)	56.6	7.5	190.7
	S15KD_R	0.44	1799	(2)	40.9	33.2	143.4
	S16KD_R	0.42	2633	(1)	59.9	2.2	167.8
	S17KD_R	0.45	1987	(5)	45.2	26.2	161.6
	S18KD_R	0.30	2215	(2)	50.4	17.7	166.7
	S19KD_R	0.35	1379	(5)	31.4	48.8	164.2
	Mean (CoV)		*2084 (0.224)*		*47.4*	*22.6*	*165.7 (0.060)*
Defective (Artificial Defect) CFRP Reinforced Beams (AD_R)	S20AD_R	-	1908	(5)	53.4	29.1	192.8
	S21AD_R	-	2051	(1)	46.6	23.8	187.3
	S22AD_R	-	1762	(5)	40.1	34.5	130.0
	S23AD_R	-	1616	(2)	36.8	40.0	153.9
	S24AD_R		2215	(1)	50.4	17.7	192.3
	Mean (CoV)		*1910 (0.123)*		*43.4*	*29.0*	*171.3 (0.164)*

(1) Tension failure for straight grained beams, (2) cross-grained tension failure, (3) ruptured at a

knot in the bottom tension lamination, (4) ruptured at the transversal cut (artificial defect) (5) CFRP debonding; * only considering knots on the beam's tension side

Table 5. Results of bending tests for large beams (wood rafters).

	Beam Number	R-ratio value*	F_u Maximum Load (kN)	Failure mode	f_m Bending Strength (MPa)	Strength Loss (%)	Flexural Stiffness $k_{1/3}$ (N/mm)
Non Defective Beams (ND)	R01ND	0.07	15.89	(2)	30.03	-	457.2
	R02ND	0.12	19.57	(1)	36.99	-	565.3
	R03ND	0.14	16.96	(2)	32.05	-	435.1
	R04ND	0.16	18.20	(2)	34.40	-	451.6
	Mean (CoV)		*17.66 (0.089)*		*33.37*	-	*477.3 (0.124)*
Defective Beams (Knot Defect, KD)	R05KD	0.24	8.75	(3)	16.54	50.4	280.1
	R06KD	0.31	11.80	(3)	22.30	33.2	264.1
	R07KD	0.36	11.81	(3)	22.32	33.1	393.8
	R08KD	0.35	9.42	(3)	17.80	46.6	329.0
	Mean (CoV)		*10.45(0.153)*		*19.74*	*40.8*	*316.8 (0.184)*
Defective (Knot Defect) CFRP Reinforced Beams (KD_R)	R09KD_R	0.30	12.45	(2)	23.53	29.5	405.4
	R10KD_R	0.33	14.75	(2)	27.88	16.5	459.6
	R11KD_R	0.25	13.38	(4)	25.29	24.2	274.5
	R12KD_R	0.31	16.17	(4)	30.56	8.4	420.1
	Mean (CoV)		*14.19 (0.114)*		*26.81*	*19.6*	*389.8 (0.205)*

(1) Tension failure for straight grained beams, (2) cross-grained tension failure, (3) ruptured at a knot in the bottom tension lamination, (4) CFRP debonding, * only considering knots on the beam's tension side

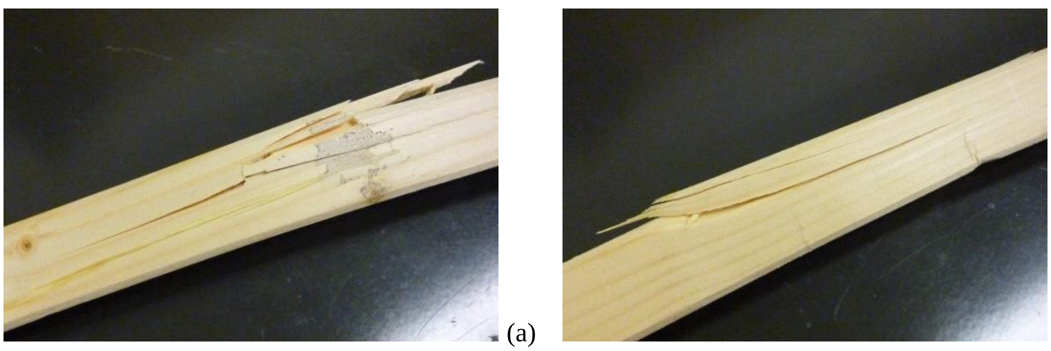

(a) (b)

Figure 10. Failure mode of non-defective beams: (a) tensile failure of timber fibres (straight-grained beams), (b) fracture propagating along the grain of timber (cross-grained tension failure).

5.3 Bending tests of defective beams

Two types of defective timber beams (artificially damaged and naturally defective timber beams) were used for testing. For naturally defective beams, the defect was in the form of a knot located about mid-span at the beam’s tension side. The ratio R of naturally defective beams was > 1/3.

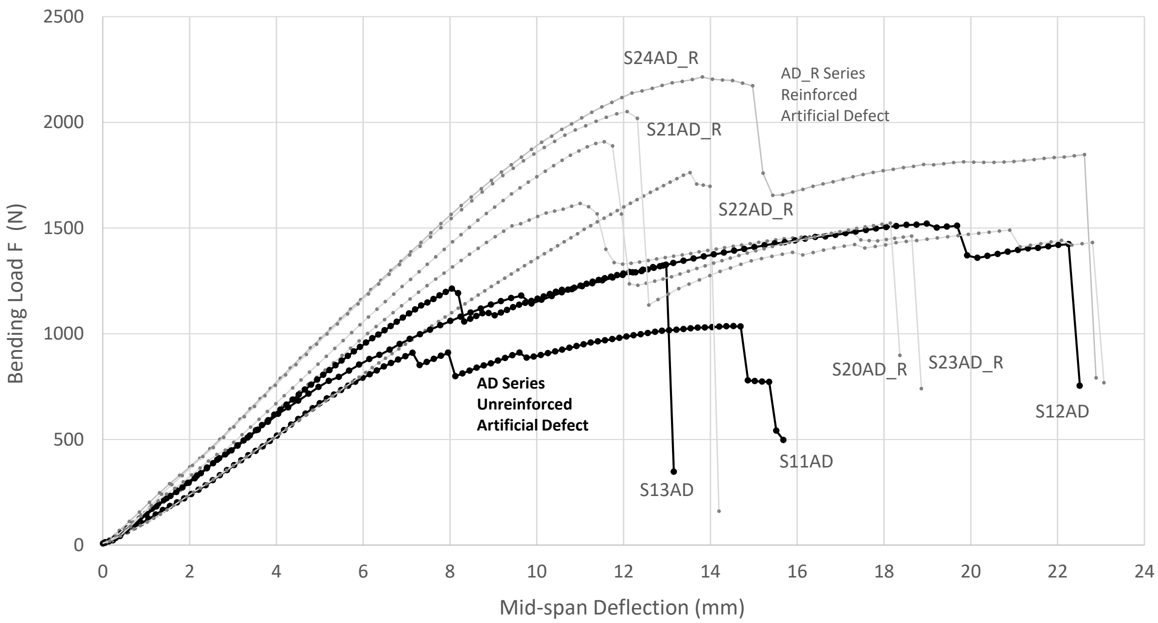

Figure 11. Four-point bending tests (simply supported ends): load versus mid-span deflection for defective (artificial defect) unreinforced (AD Series) and CFRP-reinforced (AD_R Series) small beams.

 (a)  (b)

Figure 12. Failure mode of (a) non-defective, and (b) defective large beams.

The failure mode of both types of unreinforced defective beams was governed by the defect: tension failure (cracking) initiated from the knot or from the transversal cut and a crack propagated within the timber material resulting in a cross-grained tension failure or a grain tension failure.

As expected, for both small and large beams the presence of a natural defect (a knot) on the beam tension side caused a significant reduction in both the bending load-capacity and stiffness (Fig. 11). Compared to non-defective beams, the reduction of bending capacity was 34.0% and 40.8% for small and large beams, respectively. The stiffness of large beams decreased by 33.6%. This was clearly the consequence of the discontinuity introduced in the timber by the presence of the knot. The structural response of defective beams was highly influenced by a single, localised defect: the failure of these beams always initiated from the defect itself (knot-induced mode), with cracking and fibre delamination occurring in the curved timber fibres at or near the knot (Fig. 12). The knot reduced the resisting timber section, with significant decrement of the section second moment of inertia, affecting both bending strength and stiffness.

The structural response of defective beams with the artificial defect (i.e. the transversal cut at mid-span) was easier to interpret - the overall structural response of these beams was governed by the inertial properties of the reduced cross-section over the transversal cut. This caused a reduction in capacity of 51.9%, compared to non-defective beams.

5.4 Bending tests of reinforced defective beams

Both types of defective timber beams were reinforced using a small quantity of CFRP, which was epoxy-glued over the defect to restore the continuity of timber fibres interrupted by the presence of the defect (an artificial transversal cut or a natural knot).

These beams were reinforced according to the procedure previously described and subsequently tested in the same way as for non-defective and defective beams. The results of this testing are shown in Tables 4 and 5. Unreinforced defective beams, which exhibited a poor structural response both in terms of bending capacity and stiffness during the first series of tests, performed well when tested after CFRP reinforcement, i.e. the composite material was effective in reinforcing beams, cancelling or reducing the effect of the defect. For timber rafters the bending capacity increased from 10.45 kN (defective beams) to 14.16 kN (reinforced defective beams) with an increment of 35.5%. However, the CFRP reinforcement was not able to restore the original capacity of non-defective beams (17.66 kN).

Small reinforced beams with the artificial defect performed much better - the load-capacity increased from 1.294 kN (defective beams) to 1.91 kN (CFRP-reinforced) with an increment of 47.6%. The CFRP was not able to restore the original bending capacity of non-defective beams (2.691 kN). This is not necessarily the consequence of a problem in the reinforcement mechanism, but had originated from a beam failure occurring outside the bonded area. Three failure modes of reinforced samples were recorded: 1. Debonding of the CFRP from one of the two sides of sound timber between the defect (Fig. 13a and 13c); 2. Cross-grained tension-failure, 3. Tension-failure for straight-grained beams. It is worth mentioning that the above-reported failure modes No.2 and No.3 occurred outside the bonded CFRP-reinforced area (Fig. 13b and 13d).

However, it is worth noting that delamination of the CFRP sheet was found in several tests (Figs. 13a and 13b). This is clearly an undesirable failure mode, but some discussion is necessary here to assess if actions are needed to avoid this: delamination was always observed together with timber cracking, and it is crucial to clarify if the crisis was initiated by timber cracking or delamination. In fact, if the failure initiated with FRP delamination, increasing the bonded area could effectively resolve this problem, while little can be done to avoid the failure, if this initiated from cracking in timber. In general, but not always, the failure started with FRP delamination. This typically occurred in 70% of the failure modes shown in Figures 13a and 13c.

The failure mode by CFRP-debonding could be avoided using larger CFRP sheets and more tests are necessary to address this problem, likely dependent on the dimensions of the knot, the R ratio and the type of timber. However, restoring the full bending capacity of non-defective beams is not the most important aim of this research: we believe that a balance between the need for “minimum intervention” in built heritage, as defined in the ICOMOS charter [45], (i.e., in this case, the use of small CFRP sheets) and the resulting beam capacity increment could be found. In this respect, the results of our experiment are interesting: by using a very small CFRP sheet (140 x 80 mm), it was possible to achieve 80.3% of bending capacity of non-defective beams, while this was only 59.2% for defective beams (Tab. 5).

Using the classification given in the Eurocode 5 [46], and alerting the reader about the intrinsic limitation of this conclusion, based on non-statistically significant results, we can note that the strength class of defective beams increased, after reinforcement, from C16 to C22. It worth noting that no information is available for the Young’s modulus: according to the Eurocode 5 this is 8 and 10 GPa, for C16 and C22 structural grade timber, respectively. However, test results demonstrate an increment of the flexural stiffness of reinforced beams of 22.7% (from 316.8 to 389.8 N/mm), consistent with the percentage difference between the two strength classes (25%).

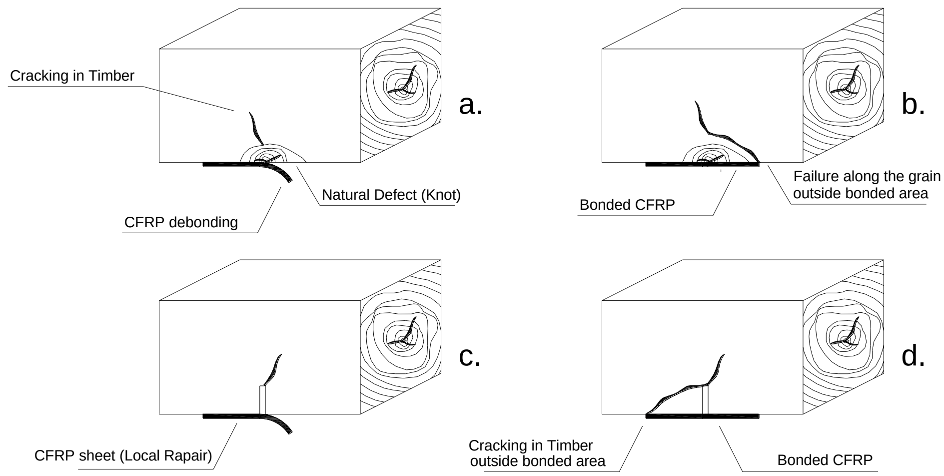

Figure 13. Failure mode of CFRP-reinforced defective beams: (a) CFRP debonding (defective beams with a natural defect) and timber cracking; (b) timber cracking along the grain outside the bonded area (defective beams with a natural defect); (c) CFRP debonding (defective beams with an artificial defect) and timber cracking; (d) timber cracking along the grain outside the bonded area (defective beams with an artificial defect).

It was expected that the application of a local CFRP reinforcement, moreover placed horizontally, should have very little effect on the stiffness properties of the timber beams under bending loads. The increment of the second moment of inertia of the reinforced section is clearly negligible. On the other hand, tests results (Tabs. 4 and 5) demonstrated some unexpected results. Figure 14 shows the load vs. mid-span deflection plot for non-defective, defective (natural defect) unreinforced and CFRP-reinforced large beams (rafters). It can be noted that the application of the CFRP reinforcement caused an increment of both the beam stiffness and the non-linear response under bending loading.

These changes can be considered as positive effects of the CFRP-reinforcement.

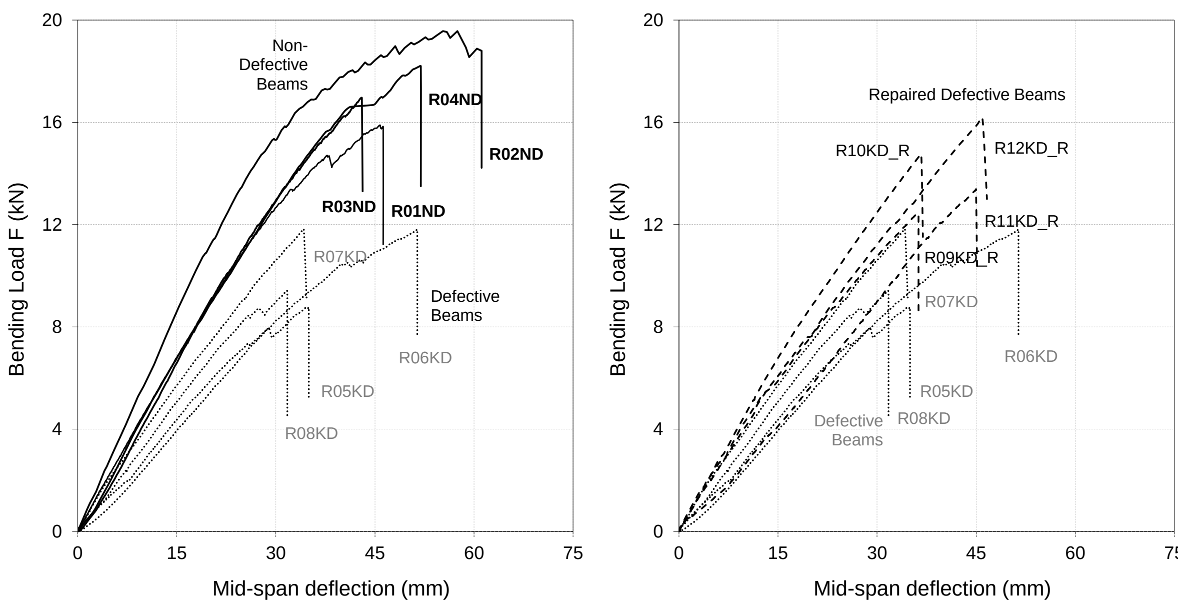

(a) (b)

Figure 14. Four-point bending tests. Load versus mid-span deflection curves: (a) for non-defective (ND Series) and defective unreinforced (KD Series) and (b) CFRP-reinforced (KD_R Series) and defective unreinforced (KD Series) large beams (rafters).

A large part of the vertical deflection of defective timber beams under bending loads, especially when the defect is a knot located on the tension side, is the consequence of the development of local cracks at the knot itself (Fig. 12b). These phenomena do not often cause the failure of the beam, but only large deflections, often increasing with time (creep behaviour). The punctual application of the CFRP sheet effectively confined the knot, preventing local cracking and deformations. This has a considerable effect not only on the bending strength, but also on the beam’s stiffness.

With regard to the non-linear response of the reinforced beams before cracking (Figs. 11 and 14), this can be attributed to several causes including: 1. Phenomena of progressive failure (slippage) of the CFRP-to-timber bonding, 2. Yielding of timber in compression. However, bond tests demonstrated that, if the epoxy was properly cured, bond failure occurred in a brittle fashion. It is therefore likely that timber beams shifted from a tensile, brittle, failure (defective beams) to a more plastic failure (CFRP-reinforced beams) initiated by yielding phenomena on the compression side of the beams. This demonstrates that the CFRP reinforcement has been effective in increasing the timber tensile strength. The critical limit state is no longer the tensile strength of the timber as the yielding compressive strength becomes the governing factor as a consequence of the CFRP reinfocement.

ANALYTICAL DESIGN

In this section, an analytical design methodology is presented for the design of non-defective, defective and FRP-reinforced beams. This method is based on the use of a modified Bazan-Buchanan model [47] for timber, which assumes a linear behaviour with brittle fracture under tensile stresses, and a bilinear material response under compressive stresses. This model allows one to calculate the ultimate moment capacity of a timber cross section on the assumptions that timber exhibits the same Young's modulus in compression and in tension and the possibility of yielding of timber in compression.

Figure 15 illustrates the typical stress-strain relationship of timber. It must be noted that timber, as a fibrous material, exhibits a higher tensile strength, however, a knot has a more serious effect in reducing the tensile rather than the compressive strength.

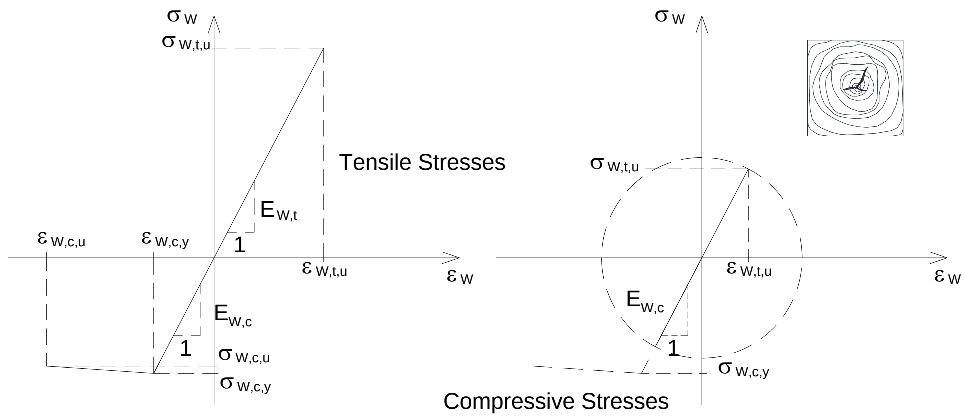

(a) (b)

Figure 15. Normal stress versus normal strain plot (along the grain): (a) Bazan-Buchanan model; (b) Likely effect of a node located on the beam tension side (tension failure): For doubly symmetric (square and rectangular) cross sections, the compressive and tensile strengths of the timber material cannot be fully exploited.

Assuming that for a non-defective beam the compressive yielding strength $\sigma_{W,c,y}$ < tensile strength $\sigma_{W,t,u}$, the calculated ultimate moment M_u must account for the plastic behaviour in compression:

$$M_u = R_{W,c1}\left[Y + \left[\frac{\left[\left(h_W - y_{N,A}\right) - Y\right]\left[2\sigma_{W,c,y} + \sigma_{W,c,u}\right]}{3\left(\sigma_{W,c,y} + \sigma_{w,c,u}\right)}\right]\right] +$$

$$+R_{W,t}\frac{2}{3}y_{N,A} + R_{W,c2}\frac{2}{3}\left[\frac{\left(h_W - y_{N,A}\right)\varepsilon_{W,c,y}}{\varepsilon_{W,c,u}}\right] \qquad (3)$$

where h_W is the height of the timber beam, $y_{N,A}$ is the vertical distance between the neutral axis and the tensile beam side, the strength and strain values are illustrated in Figure 16a, and

$$Y = \frac{\varepsilon_{W,c,y} y_{N,A}}{\varepsilon_{W,t}} \tag{4}$$

For a defective beam (with knots located on the tension side) it is very likely that $\sigma_{W,c,y} > \sigma_{W,t,u}$ and, as a result, the beam cannot deform plastically, and the ultimate moment M_u becomes (Fig. 16b):

$$M_u = R_{W,c}\frac{2}{3}\left(h_W - y_{N,A}\right) + R_{W,t}\frac{2}{3}y_{N,A} \tag{5}$$

where $R_{W,c}$ and $R_{W,t}$ are the resultant of compressive and tensile forces action on the cross section. This behaviour is also used by the Eurocode, where the design compressive strength for timber is always higher than the tensile strength for timber elements up to C30 grade [46]. As a consequence, defective timber beams do not have any excessive material strength beyond the yield value (reserve strength) and fail in a brittle manner.

For a CFRP-reinforced beam we propose to adapt the Bazan-Buchanan model. The design procedure consists of calculating two ultimate moment M_u values with one for a cross-section outside the region affected by the knot (Fig. 16a) and the other for the defective area reinforced by the application of the CFRP sheet, respectively (Fig.16b).

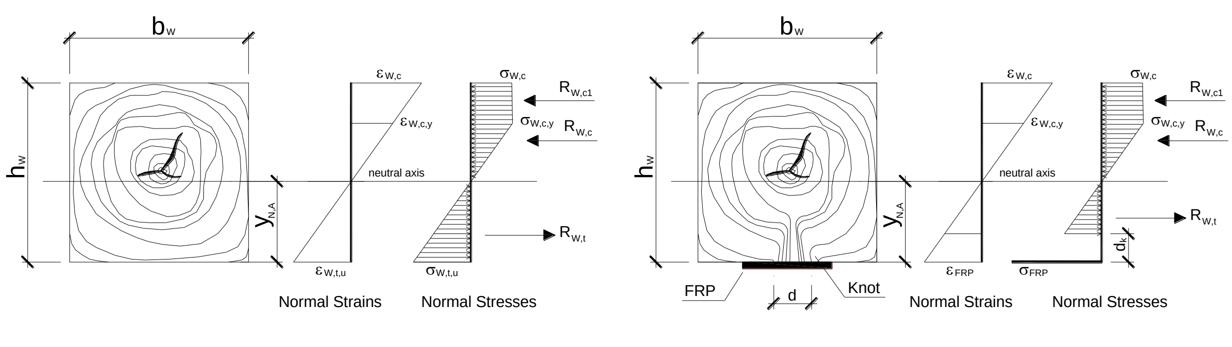

(a) (b)

Figure 16. Design method for a CFRP-reinforced beam: (a) outside the area affected by the defect; (b) area affected by the knot and CFRP-reinforced.

It is worth noting that bonding lengths (upstream and downstream of the knot) of the FRP reinforcement is a critical factor: normal stress distribution on the cross-section in Figure 16 highly depends on the ability of the bonding to transfer the stresses at interface timber-FRP. Bond test results (Section 5.1) have demonstrated a bond strength of 9.13-10.2 MPa for CFRP reinforcements. Considering the ageing effects [48-49] on the bonding and usual factors of safety, it is suggested to calculate the bonding lengths using a maximum allowable average shear stress of 3 MPa (1/3 of the bond strength), with a minimum length of the FRP sheet of three times the outer knot diameter *d* (Fig. 17). Further analysis is recommended for low-strength wood or non-smooth surfaces.

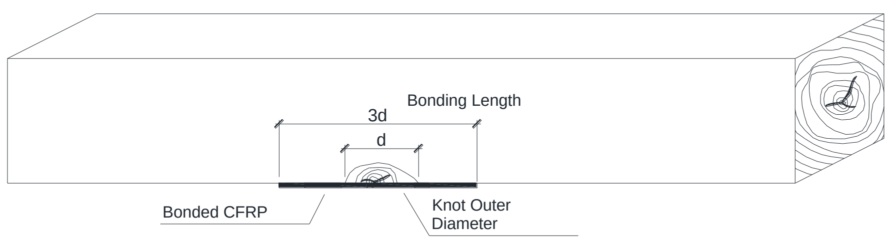

Figure 17. Calculation of the bonding length: it is suggested to use the length value using an allowable average shear stress of 3 MPa (1/3 of the bond strength), with a minimum length of the FRP sheet of three times the outer knot diameter d.

The ultimate moment M_u on the cross-section in Figure 16a can be calculated using eq. (3) for a non-defective and non-reinforced beam. For the defective section of Figure 16b, a portion of the cross-section, affected by the knot, has been neglected in the calculations.

The height d_k of this portion (Fig. 16b) was calculated, using the experimental results, and based on the following assumptions: 1. Knots initiate from the pith of the tree (Fig. 1), this is typically located near the centroid of the beam cross-section; 2. Knots do not have a significant effect on the compressive strength, 3. Considering the small FRP sheet thickness, and overall sectional area, the downward shift of the neutral axis on the section due to its application is negligible, 4. The cross sectional area affected by the knot is rectangular (Figures 2 and 16). It should be highlighted that Assumption No. 1 is only valid for large section solid timber beams (for sawn structural timber, the sawing patterns used by modern sawmills are generally designed to exclude the pith). However, this reinforcement method is clearly intended for deficient or defective solid timber beams.

The area under tensile loads $A_{W,t}$ and affected by the knot A_k are:

$$A_{W,t} = \frac{h_W}{2} b_W$$

$$A_k = \frac{h_W}{2} d \tag{6}$$

where d is the external diameter of the knot (Figs. 2 and 16), and d_k can be assumed:

$$d_k = S \frac{h_W}{4b_W} d = S \frac{h_W}{4} R \tag{7}$$

where S is a coefficient taking into account the non-uniform distribution of the stresses on the cross-section. The S value has been computed and calibrated using the experimental results, assuming a linear stress-stain response, by calculating the bending strengths f_m for unreinforced non-defective (ND series) and unreinforced defective (KD series), and by calculating the value of d_k needed to match the same bending strength of unreinforced non-defective beams. This value has been determinated using the "least-defective" beam (S04ND and R02ND for small beams and wood rafters, respectively), where the dimensions of the knot was small and its effect minimum. Table 6 shows the values of S

and d_k, resulting from its calculation using eq. (6) and (7). This table also reports the value of S computed using the average (mean) bending capacity of non-defective beams.

Table 6. Test results vs. analytical procedure.

		Experimental Tests			*Analytical Method*		
		R-ratio value	F_u Maximum Load (kN)	f_m bending strength (MPa)	*S* value		d_k value (mm)
Small Beams	S04ND	0.11	3169	72.1	-	-	-
	ND Series	0.187	2.691	61.2	-	-	-
	S07KD	0.35	1.838	41.8	0.99*	1.37	6.59
	S08KD	0.41	1.256	28.6	1.54*	1.81	10.2
	S09KD	0.45	1.456	33.1	1.17*	1.44	8.91
	S10KD	0.22	2.627	59.7	0.09*	0.83	2.51
Wood Rafters	R02ND	0.12	19.57	36.99	-	-	-
	ND Series	0.122	17.66	33.37	-	-	-
	R06KD	0.31	11.80	22.30	1.17*	1.45	22.5
	R07KD	0.36	11.81	22.32	1.01*	1.22	22.0
	R08KD	0.35	9.42	17.80	1.54*	1.75	30.8

* S calculated using average bending capacity of non-defective beams.

It can be noted that the S values are always (with the exception of S10KD) bigger than 1 (mean value 1.41). This could be considered surprising, but it is the consequence of the "trigger-effect" of a knot: knots not only reduce the resisting cross-sectional area of a beam under bending loading, but also cause a stress concentration, facilitating wood cracking or the separation of wood fibres along the grain.

The ultimate moment of the CFRP-reinforced beam is:

$$M_u = R_{W,c1}\left[Z + \left[\frac{\left[\left(h_W - y_{N,A}\right) - Z\right]\left[2\sigma_{W,c,y} + \sigma_{W,c,u}\right]}{3\left(\sigma_{W,c,y} + \sigma_{w,c,u}\right)}\right]\right] +$$

$$+R_{W,t}\frac{2}{3}\left(y_{N,A} - d_k\right) + R_{W,c2}\frac{2}{3}\left[\frac{\left(h_W - y_{N,A}\right)\varepsilon_{W,c,y}}{\varepsilon_{W,c,u}}\right] \qquad (8)$$

where

$$Z = \frac{\varepsilon_{W,c,y} y_{N,A}}{\varepsilon_{FRP}} \quad (9)$$

where $\varepsilon_{FRP} = \varepsilon_{W,t}$ is the tensile strain of the FRP.

6. CONCLUSIONS

The use of FRPs to rehabilitate structural timber has become an established practice. The speed and ease of application seems to be the key to keeping FRP retrofit cost effective. With continued research and greater implementation of FRP-based interventions in the reinforcement of timber structures, in time, the FRP material costs will come down making them even more desirable. While most of the applications to date of FRPs have been to "globally" reinforce wooden beams using FRP sheets, strips or bars applied to the beam tension side, the use of small pieces of FRP sheets to reduce the effect of local defects (mainly knots) has received relatively limited attention.

This paper described a method to reinforce locally defective timber beams with epoxy-glued CFRP. CFRP was used here to restore the continuity of the wood fibres interrupted by the presence of an artificial defect (a transversal cut) or a natural defect (a knot).

The shear properties of the FRP-to-timber bond was initially investigated. Test results have demonstrated that timber-to-FRP epoxy-bond strength is, in general, very high, ranging between 8.32 and 10.2 MPa. This strength is sometimes higher than wood-fibre-to-wood-fibre interlaminar strength, as demonstrated by the observed failure modes in bonding tests due to peeling and interlaminar debonding of wood fibres.

The main conclusions of the proposed reinforcement method for defective timber beams include:

(1) Given the high timber-to-FRP bond strength, it is possible to transfer high tensile forces from one side to the other side of the sound timber material near a defect, using very small bonded length;

(2) The application of FRPs as a local reinforcement allows achieving a better use of the mechanical resources of the composite. This is only applied in the region where tensile stresses need to be absorbed, with significant cost-savings and higher characteristics in term of “minimum intervention”. However, both creep performance and long term hygrothermal stresses need to be monitored and further investigated. These aspects highly depend on the type and quantity of resin used for the matrix.

(3) Tests results have highlighted that the presence of a knot on the tension side of a beam, in the area where the bending moment is maximum, causes a reduction of the bending capacity varying between 34% (small beams) and 41% (large beams), in comparison with non-defective beams; however, the application of the CFRP local reinforcement reduced these values to 22.5 and 19.6%, respectively. It would be fair to suggest that the use of CFRP sheets has contributed to increasing strength and stiffness of the timber element;

(4) Bending stiffness of the timber elements has increased further to the CFRP-reinforcement. The local application of the CFRP sheet confined the timber defect, preventing local cracking and deformations;

(5) The limit state of CFRP-reinforced members seems to be different from the one of defective beams. For defective beams, this was found to be the tensile strength of timber. The stress-strain response of reinforced beams was showed greater non-linearity, as a likely consequence of timber yielding in compression. It is possible to suggest that CFRP was effective in increasing timber tensile strength;

(6) Compared to a “global” reinforcement, where FRPs are typically applied to the entire tension side of the timber beams, the proposed retrofit solution provides an effective implementation of practical solutions to take into account aesthetic considerations, and an affordable reinforcement methodology which restricts the costs by using small amounts of CFRP;

(7) An initial attempt of a design procedure of the defective, FRP-reinforced, timber section has been proposed. This takes into consideration a non-tensile resistant area of a knot-affected timber section.

7. ACKNOWLEDGEMENTS

The authors wish to express their gratitude and appreciation to Matteo Romani and Alessio Molinari, who assisted greatly in making this testing possible at the Structures Laboratory of the University of Perugia, located in Terni, Italy.

8. DATA AVAILABILITY STATEMENT

The raw/processed data required to reproduce the findings of this experiment cannot be shared at this time as the data also forms part of an ongoing study.

9. REFERENCES

[1] Dinwoodie JM. (2000). Timber: its nature and behaviour. CRC Press.

[2] Fink G, Kohler J. (2014). Model for the prediction of the tensile strength and tensile stiffness of knot clusters within structural timber. European Journal of Wood and Wood Products, 72(3):331-341.

[3] Goldstein EW. (1998). Timber construction for architects and builders. McGraw-Hill Inc.

[4] Kolb J. (2008). Systems in timber engineering: loadbearing structures and component layers. Walter de Gruyter.

[5] O'Ceallaigh C, Sikora K, McPolin D, Harte A M. (2019). The mechano-sorptive creep behaviour of basalt FRP reinforced timber elements in a variable climate. Eng Struct, 200:109702.

[6] Yahyaei-Moayyed M, Taheri F. (2011). Experimental and computational investigations into creep response of AFRP reinforced timber beams. Compos struct, 93(2):616-628.

[7] Davids W G, Dagher H J, Breton J M. (2007). Modeling creep deformations of FRP-reinforced glulam beams. Wood and fiber science, 32(4):426-441.

[8] Giordano G. (1999). Tecnica delle costruzioni in legno. Hoepli, [in Italian].

[9] ISO 9709 (2018). Structural timber — Visual strength grading — Basic principles.

[10] ASTM D245 – 06 (2019). Standard Practice for Establishing Structural Grades and Related Allowable Properties for Visually Graded Lumber.

[11] Valluzzi MR. (2007). On the vulnerability of historical masonry structures: analysis and mitigation. Mat Struct, 40(7):723-743.

[12] Borri A, Corradi M. (2019). Architectural heritage: A discussion on conservation and safety. Heritage, 2(1):631-647.

[13] Gómez EP, González MN, Hosokawa K, Cobo A. (2019). Experimental study of the flexural behavior of timber beams reinforced with different kinds of FRP and metallic fibers. Compos Struct, 213:308-316.

[14] Borri A, Corradi M. (2011). Strengthening of timber beams with high strength steel cords, Compos Part B - Eng, 42:1480-1491.

[15] Soriano J, Pellis BP, Mascia NT. (2016). Mechanical performance of glued-laminated timber beams symmetrically reinforced with steel bars. Compos Struct, 150:200-207.

[16] Arriaga F, Fernandez-Cabo JL, Aira JR (2017). Timber beam bearing reinforcement with GFRP glued-in plates: Strength and hydrothermal effects, J Mater Civ Eng ASCE, 29(2):04016199.

[17] Chang WS. (2015). Repair and reinforcement of timber columns and shear walls-A review. Constr Build Mater, 97:14-24.

[18] Bertolini M, Macedo L, Almeida D, Icimoto F, Lahr F. (2013). Restoration of Structural Timber Elements Using Epoxy Resin: Analysis of Mechanical Properties, Adv Mat Res, 778:582-587.

[19] Titirla M, Michel L, Ferrier E. (2019). Mechanical behaviour of glued-in rods (carbon and glass fibre-reinforced polymers) for timber structures-An analytical and experimental study. Compos Struct, 208:70-77.

[20] Raftery GM, Kelly F. (2015). Basalt FRP rods for reinforcement and repair of timber. Compos Part B - Eng, 70:9-19.

[21] Schober KU, Harte AM, Kliger R, Jockwer R, Xu Q, Chen JF. (2015). FRP reinforcement of timber structures, Constr Build Mater, 97, 106-118.

[22] Raftery GM, Harte AM. (2011). Low-grade glued laminated timber reinforced with FRP plate, Compos Part B - Eng, 42(4):724-735.

[23] Raftery GM, Harte AM. (2013). Nonlinear numerical modelling of FRP reinforced glued laminated timber. Compos Part B – Eng, 52:40-50.

[24] Corradi M, Vo TP, Poologanathan K, Osofero AI. (2018). Flexural behaviour of hardwood and softwood beams with mechanically connected GFRP plates. Compos Struct, 206:610-620.

[25] Gilfillan JR, Gilbert SG, Patrick GRH. (2003). The use of FRP composites in enhancing the structural behavior of timber beams. J Reinf Plast Comp, 22(15):1373-1388.

[26] Corradi M, Borri, A. (2007). Fir and chestnut timber beams reinforced with GFRP pultruded Elements, Compos Part B - Eng, 38:172-181.

[27] Bank L C, Oliva M G, Bae H U, Bindrich, B. V. (2010). Hybrid concrete and pultruded-plank slabs for highway and pedestrian bridges. Constr Build Mater, 24(4):552-558.

[28] Corradi M, Borri A, Righetti L, Speranzini E. (2017). Uncertainty analysis of FRP reinforced timber beams, Compos Part B - Eng, 113:174-184.

[29] Dziuba T. (1985) The ultimate strength of wooden beams with tension reinforcement, Holzforsch Holzverw, 37:115-119.

[30] Fiorelli J, Dias AA (2003) Analysis of the strength and stiffness of timber beams reinforced with carbon fiber and glass fiber, Mat Res, 6:193-202.

[31] Buell TW, Saadatmanesh H (2005) Strengthening timber bridge beams using carbon fiber, J Struct Eng, ASCE, 131, 173-187.

[32] Borri A, Corradi M, Grazini A. (2005). A method for flexural reinforcement of old wood beams with CFRP materials, Compos Part B - Eng, 36:143-153.

[33] Nianqiang Z, Weixing S (2017). Experimental investigations of timber beams strengthened by CFRP and Rebars under bending, In IOP Conference Series: Materials Science and Engineering, 191(1): 012043.

[34] Plevris N, Triantafillou TC. (1992). FRP reinforced wood as structural material, J Mater Civ Eng ASCE, 4:300-315.

[35] Bashandy AA, El-Habashi AE, Dewedar AK (2017). Repair and strengthening of timber cantilever beams, Wood Mater Sci Eng, 13(4):241-253.

[36] Triantafillou TC. (1997). Shear reinforcement of wood using FRP materials. J Mater Civ Eng ASCE, 9:65-69.

[37] Johns KC, Lacroix S. (2000) Composite reinforcement of timber in bending, Can J Civ Eng, 27:899-906.

[38] Alam P, Ansell MP, Smedley D. (2009). Mechanical repair of timber beams fractured in flexure using bonded-in reinforcements, Compos Part B - Eng, 40:95-106.

[39] Vahedian A, Shrestha R, Crews K. (2019). Experimental and analytical investigation on CFRP strengthened glulam laminated timber beams: Full-scale experiments. Compos Part B - Eng, 164:377-389.

[40] ISO 13061-2 (2014). Physical and mechanical properties of wood — Test methods for small clear wood specimens — Part 2: Determination of density for physical and mechanical tests.

[41] ISO 13061-1 (2014). Physical and mechanical properties of wood — Test methods for small clear wood specimens — Part 1: Determination of moisture content for physical and mechanical tests.

[42] EN 408 (2010). Timber structures. Structural timber and glued laminated timber: determination of some physical and mechanical properties.

[43] ASTM D3039 (2009). Standard test method for tensile properties of fiber-resin composites.

[44] EN 13183-1 (2002). Moisture content of a piece of sawn timber. Determination by oven dry method.

[45] ICOMOS/ISCARSAH Committee. (2003). ICOMOS charter - Principles for the Analysis, Conservation and Stuctural Restoration of Architectural Heritage, Victoria Falls, Zimbabwe.

[46] Eurocode 5 (EN 1995-1-1:2004+A1) Design of timber structures - Part 1-1: General - Common rules and rules for buildings

[47] Buchanan AH. (1990). Bending strength of lumber, J Struct Eng ASCE, 116:1213-1229.

[48] Vahedian A, Shrestha R, Crews K. (2017). Effective bond length and bond behaviour of FRP externally bonded to timber. Constr Build Mater, 151:742-754.

[49] Custódio J, Cabral-Fonseca S. (2013). Advanced fibre-reinforced polymer (FRP) composites for the rehabilitation of timber and concrete structures: Assessing strength and durability. In Advanced Fibre-Reinforced Polymer (FRP) Composites for Structural Applications (pp. 814-882). Woodhead Publishing.

TABLE CAPTIONS

Table 1. Rheological and mechanical characteristics of timber beams.

Table 2. Results of mechanical characterization tests: CFRP and GFRP (CoV= Coefficient of Variation).

Table 3. Results of bonding tests.

Table 4. Results of bending tests for small beams.

Table 5. Results of bending tests for large beams (wood rafters).

Table 6. Test results vs. analytical procedure.

FIGURE CAPTIONS

Figure 1. A section of a timber beam showing the devastating effect of a knot: timber fibres are interrupted by the presence of a knot.

Figure 2. Example of a solid timber beams with knots, and the method of calculation of ratio R (external diameter of a knot d / beam smallest dimension h or b). This weakening effect is more serious when the lumber is subjected to tensile forces (typically the beam tension side).

Figure 3. Effect of earthquakes on historic buildings where timber roof beams were replaced with RC elements.

Figure 4. Different retrofitting methods using FRPs: (a) FRP sheets; (b) FRP pultruded elements at the compression side; (c) CFRP laminae.

Figure 5. Experimental testing set up: (a) small beams; (b) large beam (rafters).

Figure 6. Four-point bending: (a) small beams; (b) large beam (rafters) (dimensions in mm).

Figure 7. (a) Carbon unidirectional sheet, (b) Cutting to dimensions, (c) Application of the epoxy resin.

Figure 8. Double-lap push-pull shear test.

Figure 9. Four-point bending tests (simply supported ends): load versus mid-span deflection for unreinforced non-defective (ND Series) and defective (KD Series) small beams.

Figure 10. Failure mode of non-defective beams: (a) tensile failure of timber fibres (straight-grained beams), (b) fracture propagating along the grain of timber (cross-grained tension failure).

Figure 11. Four-point bending tests (simply supported ends): load versus mid-span deflection for defective (artificial defect) unreinforced (AD Series) and CFRP-reinforced (AD_R Series) small beams.

Figure 12. Failure mode of non-defective (a) and defective (b) large beams.

Figure 13. Failure mode of CFRP-repaired defective beams: (a) CFRP debonding (defective beams with a natural defect); (b) timber cracking along the grain outside the bonded area (defective beams with a natural defect); (c) CFRP debonding (defective beams with an artificial defect); (d) timber cracking along the grain outside the bonded area (defective beams with an artificial defect).

Figure 14. Four-point bending tests. Load versus mid-span deflection curves: (a) for non-defective (ND Series) and defective unreinforced (KD Series) and (b) CFRP-reinforced (KD_R Series) and defective unreinforced (KD Series) large beams (rafters).

Figure 15. Normal stress versus normal strain plot (along the grain): (a) Bazan-Buchanan model; (b) Likely effect of a node located on the beam tension side, producing a high reduction of the tensile strength.

Figure 16. Design method for a CFRP-reinforced beam: (a) outside the area affected by the defect; (b) area affected by the knot and CFRP-reinforced.

Figure 17. Calculation of the bonding length: it is suggested to use the length value using an allowable average shear stress of 3 MPa (1/3 of the bond strength), with a minimum length of the FRP sheet of three times the outer knot diameter *d*.